Hindawi
Journal of Nanomaterials
Volume 2023, Article ID 4213684, 7 pages
https://doi.org/10.1155/2023/4213684

Research Article

Fabrication of Visible Light Sensitive Electrospun TiO_2 Nanofibers Using Squaric Acid for Photocatalytic Application

Eba Mala Maldaye and Sathiesh Kumar Subramaniam

Jimma Institute of Technology, Jimma University, Jimma, Ethiopia

Correspondence should be addressed to Sathiesh Kumar Subramaniam; sathieshwar@gmail.com

Received 15 January 2023; Revised 15 June 2023; Accepted 20 June 2023; Published 4 July 2023

Academic Editor: Nasser Barakat

Degradation of organic pollutants using photocatalysts has gained utmost importance, due to the increasing environmental pollution. Despite various attempts to improve the photocatalytic efficiency of well-known photocatalysts such as titanium dioxide (TiO_2), by making them visible light active, various issues need to be resolved. In this work, attempts have been made to improve the visible light absorption capacities of the electrospun TiO_2 nanofibers by modification using squaric acid (SqA). An interfacial charge transfer complex is formed by the condensation reaction between the hydroxyl groups on the surface of the TiO_2 nanofibers and the SqA ligand. Various characterizations confirmed that the modification using SqA had led to the formation of the interfacial charge transfer layer, without affecting the crystallinity or morphology of the TiO_2 nanofibers. The modified TiO_2 nanofibers showed sensitivity to visible light with red shift in the optical absorption. It exhibited an improved photocatalytic efficiency of 85% against the degradation of tetracycline, compared with 60% for unmodified TiO_2 nanofibers. It also showed an increased rate of degradation of 0.21 mg/L/min, when compared with the 0.13 mg/L/min of unmodified TiO_2 nanofibers.

1. Introduction

Most of the photocatalysts available today show a response mainly to UV light. Titanium dioxide (TiO_2) is a well-known photocatalyst with a large band gap of 3.2 eV [1]. TiO_2 is widely used in organic pollutant degradation applications because of its low cost, availability, and environmental friendliness. However, due to its large band gap, TiO_2 can absorb radiations only between those small regions [2]. Inducing visible light sensitivity in such UV-active photocatalysts will improve their absorption efficiency, as the solar spectrum comprises 43% visible light. Various attempts are made earlier to improve the visible light photoactivity of TiO_2.

One such attempt was to dope nitrogen in the oxygen site of the TiO_2 to reduce the band gap [3]. The experiments revealed that the visible light responsiveness may not be due to the reduction of the TiO_2 semiconductor bandgap, but might be due to the introduction of impurity energy levels. Eventually, it increased the recombination of the photo-induced charge carriers, reducing the overall photocatalytic efficiency. This led to the search for similar other dopants to promote less energetic excitations of electrons from mid-gap dopant levels to the conduction band of TiO_2, without recombination losses. It includes doping TiO_2 with sulphur [4], red phosphorus [5], copper/iodine [6], carbon [7], and transition metals as well as loading TiO_2 with noble metals [8]. Another new approach involves the formation of an interfacial charge transfer (ICT) complex by modifying the surface of TiO_2 using organic molecules, mainly derivatives of benzene. The hydroxyl groups present in the organic molecules react with the hydroxyl groups present on the surface of the TiO_2 reacts via condensation reaction forming a covalent Ti–O–C linkage. This surface modification will aid the transfer of charges into the conduction band of TiO_2, by forming a mid-gap energy level. The alignment of energy levels of the organic–inorganic hybrid leads to a red shift, as the ground state of the ICT complex lies within the band gap of the TiO_2 [9]. There are also attempts to use nonbenzene aromatic ligands such as rhodizonic acid to from the ICT complex, which showed significant improvement in the photocatalytic efficiency of the TiO_2 [10].

In this study, a nonbenzenoid aromatic ligand, squaric acid (SqA) was used to modify the optical properties of TiO_2

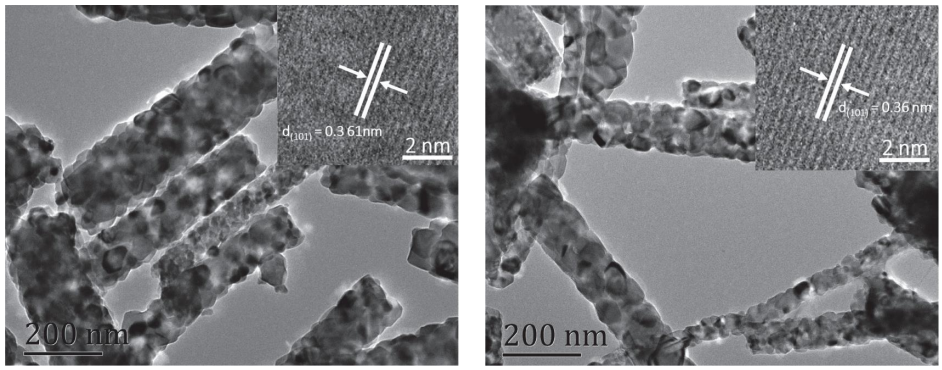

(a) (b)

FIGURE 1: TEM images of (a) TiO_2 NFs and (b) modified TiO_2 NFs. The inserts in images are HR–TEM images of the selected areas.

nanofibers (NFs). TiO_2 NFs were prepared using electrospinning and then the NFs were modified by treating with SqA [11]. The SqA-modified TiO_2 NFs were characterized using various techniques and their photocatalytic efficiency was determined by analyzing the degradation of tetracycline.

2. Experimental Section

One milliliter of tetra butyl titanate (TBT, reagent grade, 97%, Sigma) was mixed with 5 mL of ethanol (analytical grade 99.9%, Sigma) and 2 mL of acetic acid (reagent grade 99%, Sigma) and stirred for 3 hr. Then, 0.78 g of polyvinylpyrrolidone (PVP, Mw 1300000, Aladdin) and 2 mL of *N*, *N*-dimethyl formamide (DMF, for molecular biology ≥ 99%, Sigma) were added to the solution and the mixture was stirred for 12 hr. The prepared solution was electrospun using a dispensing needle of Gauge 23 as a nozzle with an injection flow rate of 1 mL/hr and a voltage of 15.6 kV. The obtained fibers were annealed at 600°C for 3 hr to remove the organic residues and produce high-purity TiO_2 NFs. The surface of the TiO_2 NFs was modified by dispersing 0.1 g of TiO_2 NFs in 30 mL of water containing 20 mg of SqA for 24 hr. Treated TiO_2 NFs were washed three times using distilled water and separated by centrifugation. The collected TiO_2 NFs were dried in a vacuum oven.

The morphology and topography of the modified TiO_2 NFs were analyzed using high-resolution transmission electron microscopy (HR–TEM). The crystallinity and phase of the fibers were analyzed using an X-ray diffractometer (XRD). Significant X-ray photoelectron spectroscopy structural changes and the electron distribution of modified TiO_2 NFs were investigated using a Raman spectrometer and electron paramagnetic resonance (EPR) spectrometer. EPR spectra of the solid samples were recorded at room temperature using X-band microwave frequency of 9.5 GHz with modulation frequency of 100 kHz, modulation amplitude of 10 G, and constant microwave power of 1.2 mW. Optical properties were studied by diffused reflectance spectrum using UV–Visible spectrometer. X-ray photoelectron spectroscopy (XPS) was recorded using one color Al Kα radiation (225 W, 15 mA, 15 kV) with a spot size of 100 mm. The photocatalytic efficiencies of TiO_2 NFs and SqA-modified TiO_2 NFs were analyzed by comparing their ability to degrade tetracycline organic dye under 300 W Xenon lamp. The photocatalyst was dispersed in 100 mL aqueous solution of tetracycline at the concentration of 20 mg/L. Next, the dispersion was stirred magnetically in the dark until the adsorption–desorption equilibrium is achieved, by measuring the change in concentration of tetracycline at an interval of 20 min. Then, the dispersion was irradiated using the Xenon lamp and the photocatalytic activity was measured by measuring the degradation of tetracycline at an interval of 20 min, using UV–Visible spectrometer (by measuring the adsorption peak of tetracycline at 357 nm).

3. Results and Discussion

HR-TEM TiO_2 NFs and SqA surface-modified TiO_2 NFs are shown in Figures 1(a) and 1(b), respectively. Both images have similar shapes and morphology, which implies that the surface modification does not induce any morphological changes in the TiO_2 NFs. The image also reveals the presence of nanometer-sized grains of TiO_2 in both samples. The insert in the figures indicates the lattice spacing of the TiO_2 NFs and modified TiO_2 NFs, both have a lattice spacing corresponding to the (101) anatase phase of TiO_2. The occurrence of impurities or any other crystalline phases were not found in both samples.

XRD pattern of the TiO_2 NFs and modified TiO_2 NFs is shown in Figure 2(a). Both the samples have similar diffraction peaks and the peaks at 25.0°, 37.6°, 47.7°, 53.7°, 54.7°, and 62.4° can be, respectively, indexed to (101), (004), (200), (105), (211), and (204) crystal planes. These patterns were indexed to the tetragonal anatase phase of TiO_2 (JCPDS: 21-1272) [12]. These XRD results agree with the transmission electron microscopy (TEM) images that there were no impurities and any other crystalline phases. The Raman spectra of the TiO_2 NFs and modified TiO_2 NFs are compared in Figure 2(b). Both the samples showed resonance peaks at 197, 395, 514, and 634 cm^{-1}, which correspond to the Ti–O bands in the anatase phase of TiO_2 [13]. However, the strongest peak at 142 cm^{-1} for the pristine TiO_2 NFs had shifted to

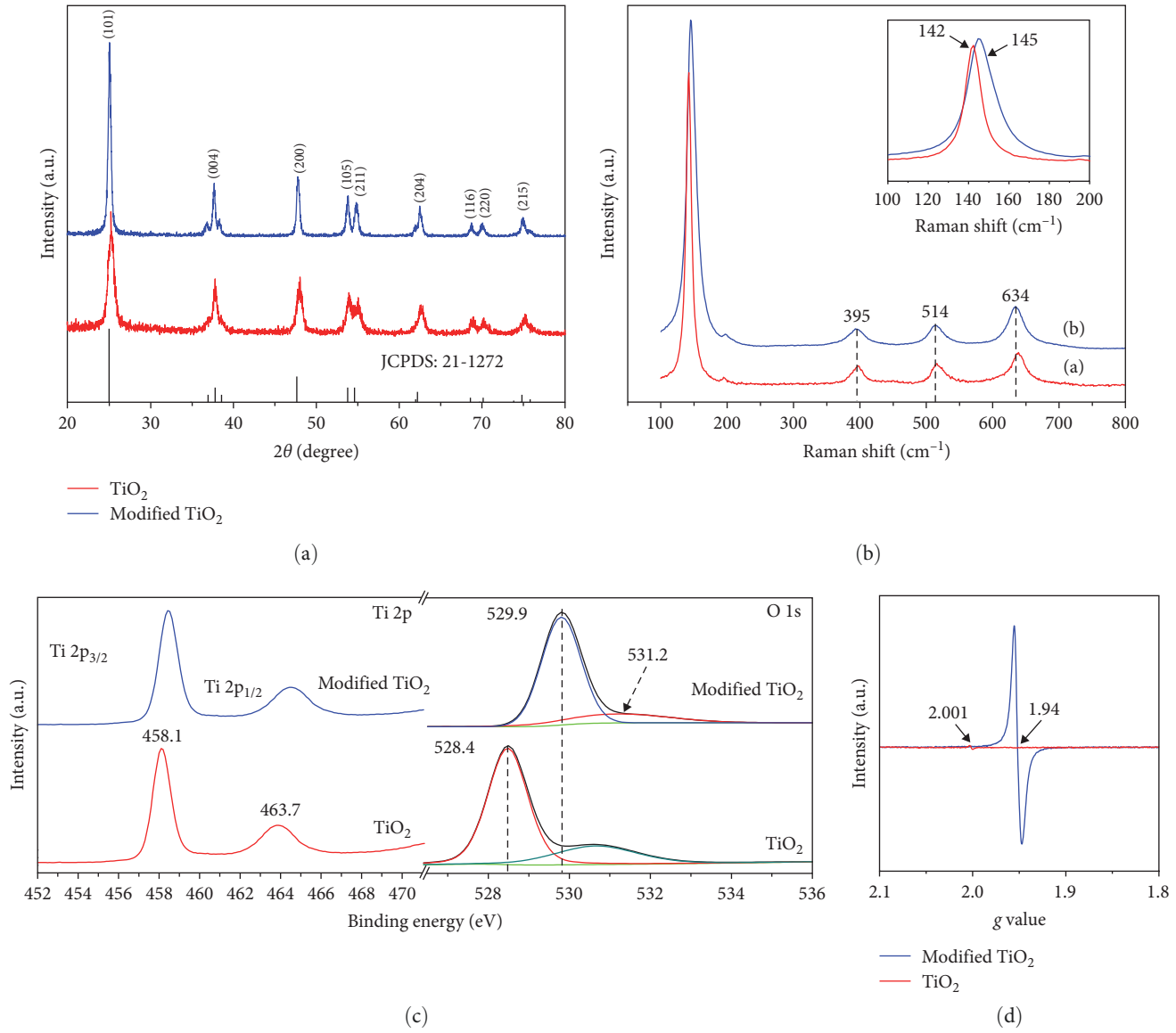

FIGURE 2: (a) X-ray diffraction pattern, (b) Raman spectra, (c) X-ray photoelectron spectra, and (d) electron paramagnetic resonance spectra.

145 cm^{-1} after the surface modification using SqA. This peak shift and broadening shall be due to the presence of Ti^{3+} species and the induction of more oxygen vacancies [14]. In addition, a slight increase in the intensity of the strongest peak and peak broadening of the modified TiO_2 NFs when compared with the TiO_2 NFs shall be attributed to the increase in the number of oxygen vacancies in the lattice of modified TiO_2 NFs, due to the introduction of nonbenzenoid aromatic ligand by SqA [15].

XPS spectrum of the samples corresponding to O 1s and Ti 2p is shown in Figure 2(c). The strong peak at the 528.4 eV of the TiO_2 NFs corresponds to the lattice oxygen of Ti–O, whereas the strong peak (529.9 eV) of modified TiO_2 NFs had a positive shift of ~1.27 eV. Han et al. [16] reported a shift of O 1s peaks of the H_2O_2-modified TiO_2 toward a lower energy side, which they had attributed to the presence of more number of O atoms than Ti atoms in the lattice. In this work, the peak had shifted to a higher energy side, which can be attributed to the lesser number of O atoms than Ti atoms in the lattice (presence of oxygen vacancies). A small new peak found at 531.2 eV of modified TiO_2 NFs can be due to the presence of surface hydroxyl groups (Ti–OH) [17, 18]. Ti 2p spectra of both TiO_2 NFs and modified TiO_2 NFs showed two similar peaks at 458.1 and 463.7 eV, respectively, which can be assigned to the Ti^{4+} oxidation state. However, no additional peaks for Ti^{3+} species were observed in the modified TiO_2 NFs, which is in contrast to the Raman spectroscopy. This suggests the formation of a shell-like structure on the surface of the modified TiO_2 NFs, which was dominated by the Ti^{4+} species. Whereas, Ti^{3+} species were present in the inner core of the modified TiO_2 NFs. The thickness of the shell-like structure should have been more than (5 nm)

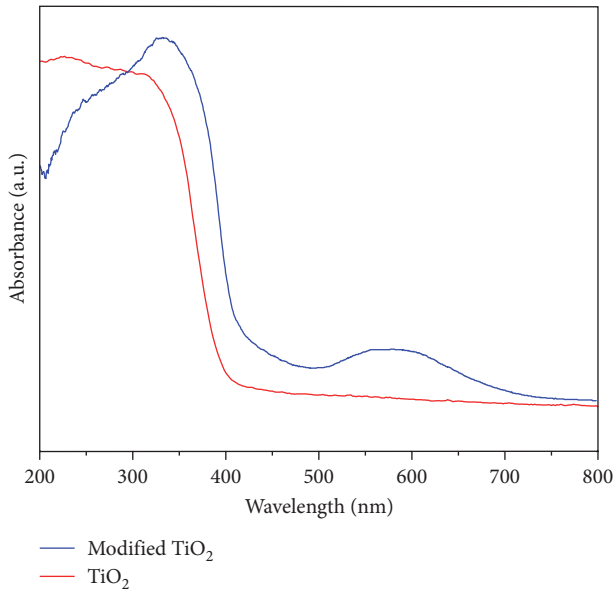

Figure 3: Diffused reflectance spectra of pristine and modified TiO_2.

the detection limit of XPS [15]. To confirm the formation of such core/shell structure, the samples were analyzed using EPR spectroscopy.

EPR spectra of the TiO_2 NFs and modified TiO_2 NFs are shown in Figure 2(d). TiO_2 NFs do not show any paramagnetic signal, whereas modified TiO_2 NFs showed strong g values at ~1.94, which confirms the presence of paramagnetic Ti^{3+} species [19, 20]. In general, the occurrence of Ti^{3+} will be followed by the formation of oxygen vacancies. However, no signals were found at 2.005, which suggests that there were no Ti^{3+} species at the surface [17, 20]. Hence, it is inferred in connection with the XPS and Raman spectra data that the Ti^{3+} species and corresponding oxygen vacancies exist in the bulk rather than on the surface of modified TiO_2 NFs. Thus, in the modified TiO_2 NFs, oxygen vacancies exist in the core with TiO_2 as a shell. This also backs the formation of an ICT complex, which in turn will enhance the absorption of lower energy visible light spectrum in modified TiO_2 NFs.

The UV–Visible diffused reflectance spectrum of the samples is shown in Figure 3. The pristine TiO_2 NFs exhibit a sharp absorption at 400 nm [21] without any significant absorption in the visible and near infrared region. While the modified TiO_2 NFs, which were brown in color when compared with the white color of pristine TiO_2 NFs, displayed a broad absorption in the 400–700 nm region. A significant red shift of 300 nm (1.3 eV) was observed for the modified TiO_2 NFs, as the absorption onset for modified TiO_2 NFs was at 700 nm when compared with that of the pristine TiO_2 NFs, which was at 400 nm. This broadening of the optical absorption can be attributed to the induction of oxygen deficiencies in the subband excitation near the conduction band leading to the formation of the ICT region. Formation of the ICT complex significantly improved the optical absorption of the modified TiO_2 NFs. The hydroxyl groups on the SqA molecule interact with the surface of TiO_2 NFs through coordination bonding. This process led to the formation of a strongly bonded monolayer of SqA molecules on the surface of the TiO_2 NFs, altering the surface properties of the TiO_2. This SqA acts as a sensitizer, injecting electrons into the conduction band of the TiO_2 semiconductor through the ICT complex [22, 23]. The actual mechanism involves the formation of hydroxyl radicals (˙OH) on the surface of SqA-treated TiO_2 NFs under light irradiation. Upon absorbing a photon, the ICT complex undergoes excitation. The energy from the absorbed photon promotes an electron from the highest occupied molecular orbital of the SqA to the lowest unoccupied molecular orbital of TiO_2, leading to the formation of electron–hole pairs. This excitation process is facilitated by the strong electronic coupling between the SqA and TiO_2. These electron–hole pairs then react with water and oxygen adsorbed on the TiO_2 surface to form hydroxyl radicals (·OH). The hydroxyl radicals are highly reactive and attack the tetracycline molecules, leading to their degradation into smaller, less harmful compounds.

The photocatalytic activity of the samples against tetracycline is shown in Figure 4. Spectroscopic measurements of the concentration of tetracycline in dark conditions revealed that the sorption–desorption equilibrium between the photocatalyst and the tetracycline was achieved between 40 and 60 min. Therefore, all the dispersions of photocatalyst and tetracycline were stirred in the dark conditions for 60 min, before exposing them to the Xenon illumination. Reduction in the concentration of the tetracycline was observed for both samples. However, modified TiO_2 NFs exhibited a drastic degradation efficiency against tetracycline when compared with pristine TiO_2 NFs. SqA creates carboxylic acid groups on the TiO_2 surface. This modification not only enhances the separation of electron–hole pairs but also reduces recombination and increases the efficiency of photocatalytic degradation. In addition, the carboxylic acid groups can also act as active sites for adsorption of tetracycline molecules, leading to their degradation by the generated reactive oxygen species.

The rate of degradation for blank, TiO_2 NFs, and modified TiO_2 NFs at dark and illuminated conditions is shown in Figure 4(c). No reduction in the concentration was observed in the blank solution without any photocatalyst, both in dark and illuminated conditions. In dark conditions, TiO_2 NFs and modified TiO_2 NFs removed 4% and 16% of the tetracycline, respectively, in 60 min by absorption. Whereas under illuminated conditions, the TiO_2 NFs and modified TiO_2 NFs exhibited degradation efficiencies of 60% and 85%, respectively, in 80 min. Modified TiO_2 NFs have also showed an increased rate of degradation of 0.21 mg/L/min, when compared with the 0.13 mg/L/min of unmodified TiO_2 NFs. This increase in the photocatalytic efficiency of modified TiO_2 NFs can be attributed to the absorption of more photons in the visible region by the modified TiO_2, due to the presence of an ICT layer as shown in Figure 4(d). This ICT complex was a result of the condensation reaction between the hydroxyl groups in SqA and the surface hydroxyl groups in the TiO_2 NFs, forming the Ti–O–C linkage [10].

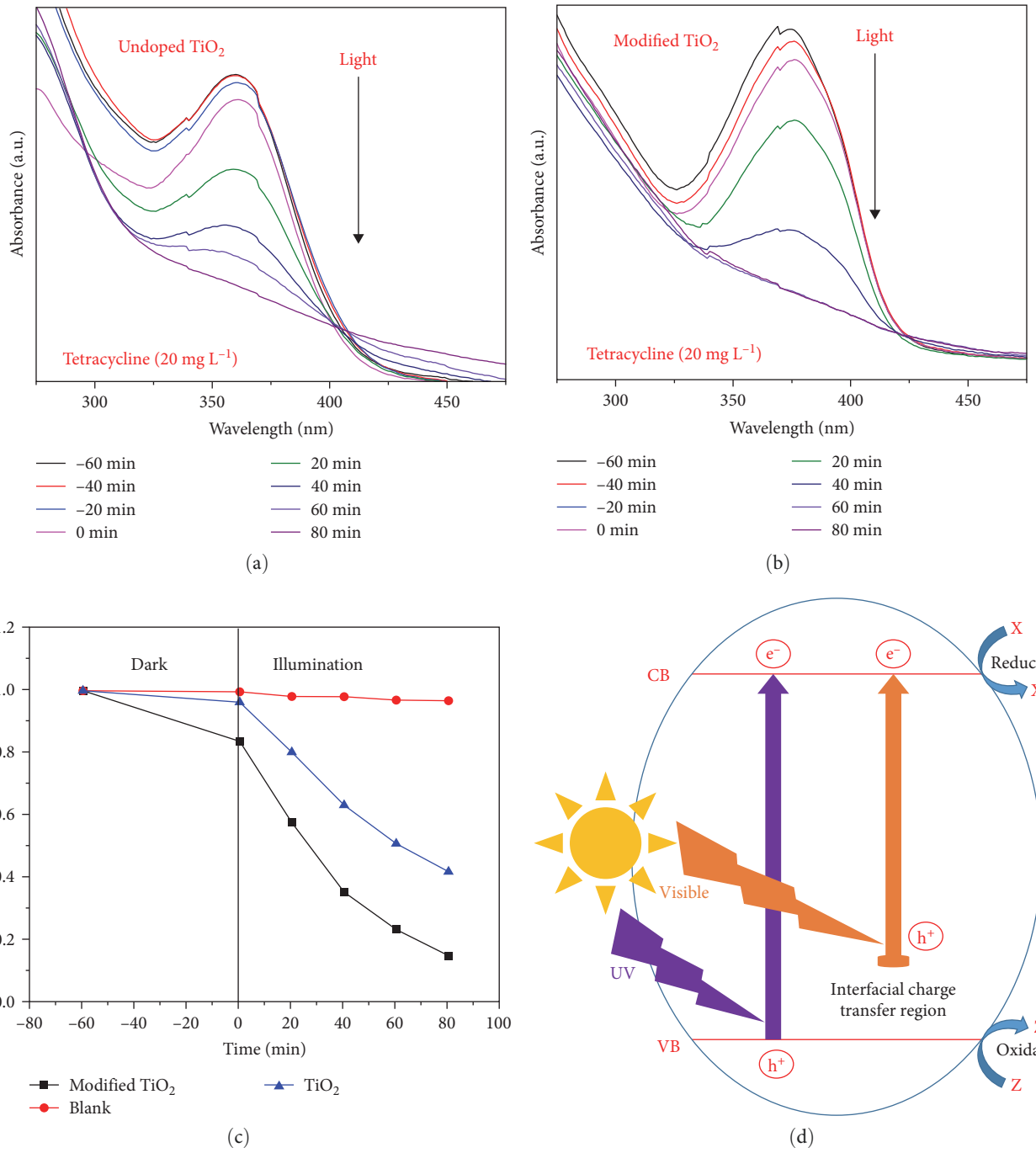

Figure 4: Continued.

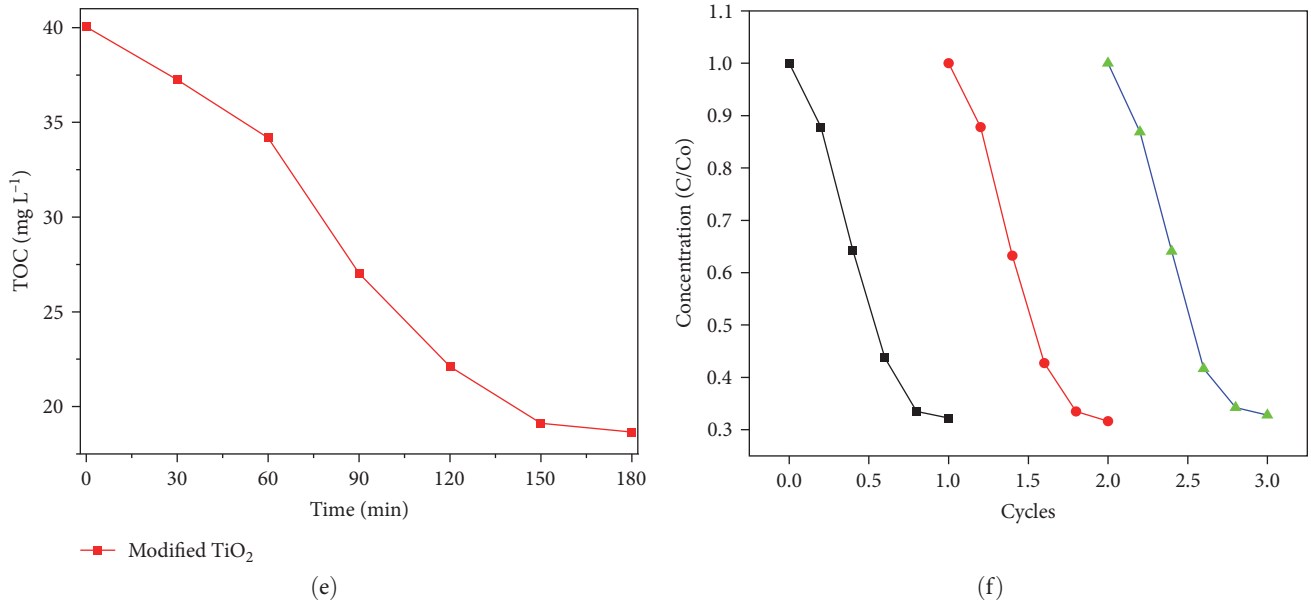

FIGURE 4: Photocatalytic degradation of tetracycline by (a) pristine TiO_2 NFs, (b) modified TiO_2 NFs, (c) rate of photocatalytic degradation in dark and illuminated conditions, (d) schematic illustration of the energy alignment in modified TiO_2 NFs, (e) rate of degradation of total organic carbon by modified TiO_2 NFs, and (f) recycle efficiency of the modified TiO_2 NFs.

Tetracycline was used as a typical persistent organic pollutant and its mineralization was determined by measuring total organic carbon (TOC). Modified TiO_2 NFs (200 mg) were used to degrade tetracycline under illumination and the TOC was measured at a regular interval of 30 min and shown in Figure 4(e). A 47% decrease in the TOC was observed, which exhibits the efficiency of the modified TiO_2 NFs to mineralize the tetracycline into H_2O and CO_2.

Furthermore, recycling efficiency of the modified TiO_2 NFs was analyzed by separation, washing, and reusing the photocatalyst in multiple cycles. The results are shown in Figure 4(f). Ninety-one percent efficiency was observed in the first cycle and it further stayed consistent at 84% over three cycles.

4. Conclusions

The modification of electrospun TiO_2 NFs using SqA has significantly improved the absorption efficiency of the NFs in the visible spectrum by the formation of the ICT complex. It should also be noted that the modification does not create any changes in the morphology or crystallinity of the TiO_2 NFs. The photocatalytic efficiency of the modified TiO_2 NFs against the tetracycline was significantly higher than that of the pristine TiO_2 NFs, which can be attributed to the formation of the ICT complex by condensation of hydroxyl groups. This proves and opens up the possibility of using organic ligands to enhance the visible light activity of the higher band gap photocatalysts.

Data Availability

The data that support the findings of this study are available, upon reasonable request, from the corresponding author.

Conflicts of Interest

The authors declare that they have no conflicts of interest.

Acknowledgments

The authors thank the World Bank–MAPRONANO ACE, Makerere University for partial funding to this work.

References

[1] F. E. Osterloh, "Inorganic materials as catalysts for photochemical splitting of water," *Chemistry of Materials*, vol. 20, no. 1, pp. 35–54, 2008.

[2] A. L. Linsebigler, G. Lu, and J. T. Yates Jr., "Photocatalysis on TiO_2 surfaces: principles, mechanisms, and selected results," *Chemical Reviews*, vol. 95, no. 3, pp. 735–758, 1995.

[3] S. Du, J. Lian, and F. Zhang, "Visible light-responsive N-doped TiO_2 photocatalysis: synthesis, characterizations, and applications," *Transactions of Tianjin University*, vol. 28, pp. 33–52, 2022.

[4] T. Ohno, M. Akiyoshi, T. Umebayashi, K. Asai, T. Mitsui, and M. Matsumura, "Preparation of S-doped TiO_2 photocatalysts and their photocatalytic activities under visible light," *Applied Catalysis A: General*, vol. 265, no. 1, pp. 115–121, 2004.

[5] S. A. Ansari and M. H. Cho, "Highly visible light responsive, narrow band gap TiO_2 nanoparticles modified by elemental red phosphorus for photocatalysis and photoelectrochemical applications," *Scientific Reports*, vol. 6, Article ID 25405, 2016.

[6] M. Dorraj, B. T. Goh, N. A. Sairi, P. M. Woi, and W. J. Basirun, "Improved visible-light photocatalytic activity of TiO_2 co-doped with copper and iodine," *Applied Surface Science*, vol. 439, pp. 999–1009, 2018.

[7] Z. Wu, F. Dong, W. Zhao, H. Wang, Y. Liu, and B. Guan, "The fabrication and characterization of novel carbon doped TiO_2 nanotubes, nanowires and nanorods with high visible light

photocatalytic activity," *Nanotechnology*, vol. 20, no. 23, Article ID 235701, 2009.

[8] V. Etacheri, C. Di Valentin, J. Schneider, D. Bahnemann, and S. C. Pillai, "Visible-light activation of TiO_2 photocatalysts: advances in theory and experiments," *Journal of Photochemistry and Photobiology C: Photochemistry Reviews*, vol. 25, pp. 1–29, 2015.

[9] B. Milićević, V. Đorđević, D. Lončarević, S. P. Ahrenkiel, M. D. Dramićanin, and J. M. Nedeljković, "Visible light absorption of surface modified TiO_2 powders with bidentate benzene derivatives," *Microporous and Mesoporous Materials*, vol. 217, pp. 184–189, 2015.

[10] Y. Sun, J. B. Mwandeje, L. M. Wangatia, F. Zabihi, J. Nedeljković, and S. Yang, "Enhanced photocatalytic performance of surface-modified TiO_2 nanofibers with rhodizonic acid," *Advanced Fiber Materials*, vol. 2, pp. 118–122, 2020.

[11] E. M. Maldaye, "Synthesis and characterization of Squaric acid surface modified electrospun TiO_2 nanofiber for photocatalytic application," Unpublished Master's Thesis, Jimma University, Ethiopia, 2020.

[12] C. Chen, X. Hu, B. Zhang, L. Miao, and Y. Huang, "Architectural design and phase engineering of N/B-codoped TiO_2(B)/anatase nanotube assemblies for high-rate and long-life lithium storage," *Journal of Materials Chemistry A*, vol. 3, no. 45, pp. 22591–22598, 2015.

[13] A. G. Ilie, M. Scarisoareanu, I. Morjan, E. Dutu, M. Badiceanu, and I. Mihailescu, "Principal component analysis of Raman spectra for TiO_2 nanoparticle characterization," *Applied Surface Science*, vol. 417, pp. 93–103, 2017.

[14] X. Chen, L. Liu, P. Y. Yu, and S. S. Mao, "Increasing solar absorption for photocatalysis with black hydrogenated titanium dioxide nanocrystals," *Science*, vol. 331, no. 6018, pp. 746–750, 2011.

[15] Q. Zhu, Y. Peng, L. Lin et al., "Stable blue TiO_{2-x} nanoparticles for efficient visible light photocatalysts," *Journal of Materials Chemistry A*, vol. 2, no. 12, pp. 4429–4437, 2014.

[16] E. Han, K. Vijayarangamuthu, J.-S. Youn, Y.-K. Park, S.-C. Jung, and K.-J. Jeon, "Degussa P25 TiO_2 modified with H_2O_2 under microwave treatment to enhance photocatalytic properties," *Catalysis Today*, vol. 303, pp. 305–312, 2018.

[17] M. Xing, W. Fang, M. Nasir, Y. Ma, J. Zhang, and M. Anpo, "Self-doped Ti^{3+}-enhanced TiO_2 nanoparticles with a high-performance photocatalysis," *Journal of Catalysis*, vol. 297, pp. 236–243, 2013.

[18] R. Kumar, S. Govindarajan, R. K. S. K. Janardhana, T. N. Rao, S. V. Joshi, and S. Anandan, "Facile one-step route for the development of in situ cocatalyst-modified Ti^{3+} self-doped TiO_2 for improved visible-light photocatalytic activity," *ACS Applied Materials & Interfaces*, vol. 8, no. 41, pp. 27642–27653, 2016.

[19] N. Yu, Y. Hu, X. Wang et al., "Dynamically tuning near-infrared-induced photothermal performances of TiO_2 nanocrystals by Nb doping for imaging-guided photothermal therapy of tumors," *Nanoscale*, vol. 9, no. 26, pp. 9148–9159, 2017.

[20] F. Zuo, L. Wang, T. Wu, Z. Zhang, D. Borchardt, and P. Feng, "Self-doped Ti^{3+} enhanced photocatalyst for hydrogen production under visible light," *Journal of the American Chemical Society*, vol. 132, no. 34, pp. 11856-11857, 2010.

[21] O. Solcova, T. Balkan, Z. Guler, M. Morozova, P. Dytrych, and A. S. Sarac, "New preparation route of TiO_2 nanofibers by electrospinning: spectroscopic and thermal characterizations," *Science of Advanced Materials*, vol. 6, no. 12, pp. 2618–2624, 2014.

[22] Z. Barbieriková, M. Šimunková, V. Brezová et al., "Interfacial charge transfer complex between TiO_2 and non-aromatic ligand squaric acid," *Optical Materials*, vol. 123, Article ID 111918, 2022.

[23] I. A. Janković, Z. V. Šaponjić, M. I. Čomor, and J. M. Nedeljković, "Surface modification of colloidal TiO_2 nanoparticles with bidentate benzene derivatives," *The Journal of Physical Chemistry C*, vol. 113, no. 29, pp. 12645–12652, 2009.